Eur. Phys. J. Special Topics **227**, 883–893 (2018)

https://doi.org/10.1140/epjst/e2018-800015-1

THE EUROPEAN PHYSICAL JOURNAL SPECIAL TOPICS

Regular Article

Synchronization structure of evolving epileptic networks using cross-entropy

Abner Cardoso Rodrigues[1], Luis Otavio Sales Ferreira Caboclo[2], Hilda Alicia Cerdeira[3,4], Edson Amaro Jr.[2], and Birajara Soares Machado[2,a]

[1] Instituto de Matemática e Estatística, Universidade de São Paulo, São Paulo, Brazil
[2] Hospital Israelita Albert Einstein, São Paulo, Brazil
[3] São Paulo State University (UNESP), Instituto de Física Teórica, São Paulo, Brazil
[4] Epistemic, Department of Research, São Paulo, Brazil

Received 1 February 2018 / Received in final form 27 April 2018
Published online 19 October 2018

Abstract. In this paper we present connectivity patterns of evolving large scale epileptic networks. We employed a cross-entropy measure in the frequency domain on EEG signals to infer the networks, before and during episodes of epileptic seizures. This measure allowed us to make a richer portrait about the node interactions on the graph and to identify emergent structures associated with the synchronization of brain activity. Our results points to a more complex scenario of network organization than the synchronized/unsynchronized dichotomy, with two main results: first, showing regions with unsynchronized (or independent) behavior, even during absence seizures, contradicting the concept of hypersynchrony. Furthermore, we explore the cross-entropy fluctuations along the seizure: a group of nodes became more similar over time while another group became more different, showing a complementary behaviour and different local brain activities. These results bring new questions about the spreading and the sustenance of the epileptic seizures and others synchronization phenomena in living systems.

1 Introduction

Epilepsy was characterized by a hypersynchronous state between cortical regions [1], but recent advances in complex networks and nonlinear theory are showing a more dynamical behaviour characterized by intervals of synchronous and asynchronous states during the course of the seizure [2,3]. Several studies reported desynchronization state can be found in the first stages of seizure onset (see, for instance, Mormann et al. [4], Wendling et al. [5] and Schindler et al. [6]) and a more synchronized state can be found as the seizure progresses (see Schindler et al. [6] and Jiruska et al. [7]). Simulation studies also reported that weak levels in synchronization can be found during seizures, depending on the network parameters [8,9]. Moreover, the seizure can start as a microseizure in the focal zone [10,11] or through multiple distant microseizures

[a] e-mail: birasm@gmail.com

[7,12]. In both cases, there are regions generating the ictal activity whereas other regions are not affected, resulting in a decrease in synchronous state [13].

Despite these recent advances that show a more complex synchronization scenario during epileptic seizures, the role of each node in the phenomena still poorly understood. How to identify the regions that are increasing the global synchronization? How to identify the role of a region along time? To help to answer these questions we are proposing the use of a cross-entropy measure in frequency domain. We show that this measure can be useful to identify different behaviors of the nodes during a episode of seizure.

More specifically, we inferred the networks during absence seizures which is kind of epilepsy were the presence of the seizure onset zone is unclear and the synchronization emerges abruptly and globally [14]. We show two different patterns which can be found during generalized epilepsy: most part of the cortex exhibits similar behaviour while a few cortical regions shows a very different brain activity, unsynchronized with the global state. These observations contradict the notion of hypersynchrony in absence epilepsy (see Amor et al. [15] and Visani et al. [16]) and point out a novel description of the dynamics of absence seizures. Secondly, the pairwise cross-entropy fluctuate considerably along the course of the seizure, in which the differences or similarities among the brain activity signals are dynamically changing over time. Furthermore, as this measure can label which brain regions have similar activity, it can help avoiding spending time and resources in irrelevant data, for example using more electrodes when a small subset can well capture the phenomena.

Understanding the behaviour of the nodes during epileptic seizures can also be helpful to improve artificial models of epilepsy [17,18]. For example, Panahi et al. [18] proposed a model of epilepsy based on chaotic artificial neural network, in this model the transition to a epileptic state is possible for some values in the neurons variables. In Martinet et al. [19] a multiscale model for epilepsy was proposed considering the ions concentration and the resulting brain activity signal. Adding another scale to these models, i.e. the network description, estimated for example with cross-entropy measure, can lead to a more realistic model. In this way, the knowledge combined about dynamical properties of the brain and the connectivity can be useful to provide more realistic models in this research field.

2 EEG data

Typical absence seizures, which a remarkable feature is the lack of motor manifestation, were recorded and analyzed in this study. EEG recordings were acquired on 32-channel digital amplifier (Ceegraph, Bio-logic Systems Corp, Illinois/USA) with sampling rate of 256 Hz. The recordings are from a few minutes to almost an hour. Scalp electrodes were placed according to the 10–20 International System. The EEG records were acquired with a high-pass filter of 1 Hz and a low-pass filter of 70 Hz. Notch filter (60 Hz) was applied whenever deemed necessary. Waking and sleep recordings were obtained from all patients. Hyperventilation and intermittent photic stimulation were performed routinely. The raw data were reviewed and ictal period was marked by a board-certified clinical neurophysiologist. In Figure 1 we show a example of EEG data transition from interictal to ictal states.

The study did not include patient interventions and the analysis was based on anonymised retrospective data and, as such, we did not seek ethics committee approval. EEG data from eight patients were recorded by the authors, all children and adolescents diagnosed with absence seizures.

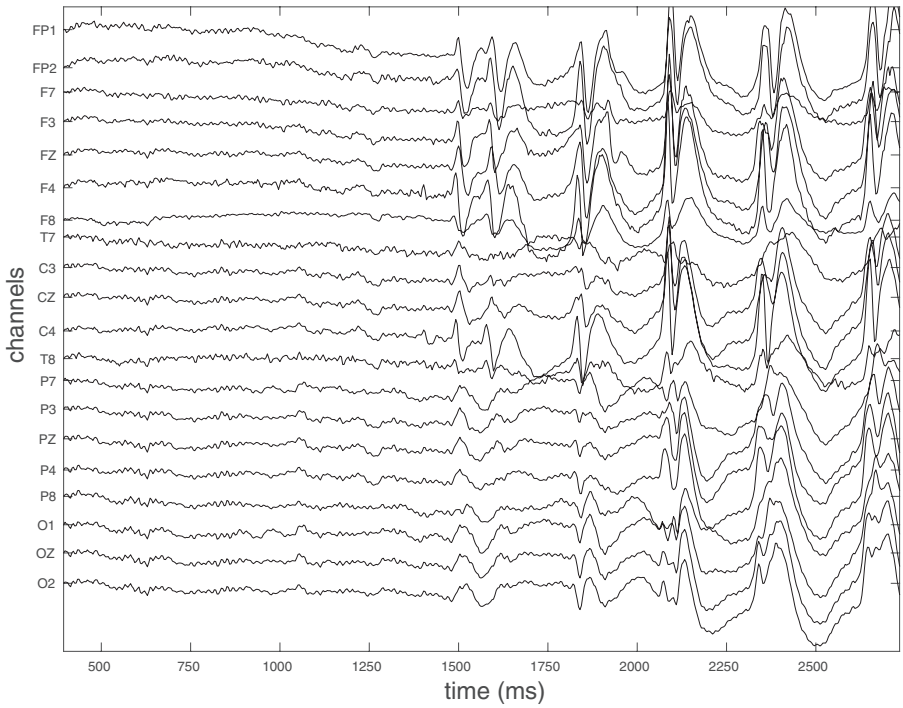

Fig. 1. Example of EEG multivariate data from a patient during the start of an absence seizure (around 1750 ms). The seizure is characterized by an amplitude increases and the spike-wave complexes that can be seen clearly in frontal electrodes (FP1, FP2, F3, F4, F7 and FZ). A desirable characteristic observed in EEG data from absence seizure is the lack of artifacts caused by eye and motor movements.

3 Methods

We adapted a measure derived from information theory, the cross-entropy, to the frequency domain in order to analyze EEG data from patients with absence seizures. In this section we will introduce this measure and an application in a toy model. Additionally, as we analyzed the weighted network without pruning the connections, we implemented a procedure to identify the relevant nodes. In this way, we can investigate only the expressive regions in the brain connectivity.

3.1 Kullback–Leibler divergence in frequency domain

The Kullback–Leibler divergence (KLD) is an asymmetric measure of the difference of information between two probability distributions [20]. Considering two probability distributions F and G, this measure is defined $D_{\mathrm{KL}}(F,G) = \int f(x) \ln \frac{f(x)}{g(x)} dx$, where f and g denote the probability densities of F and G, respectively. Therefore, $D_{\mathrm{KL}}(F,G) \geq 0$ and measures the information difference when F is compared with the reference probability distribution G. It is possible to define the cross-entropy in terms of D_{KL} [20] by the relation $H(F,G) = D_{\mathrm{KL}}(F,G) + H(F)$, where $H(F) = -\int f(x) \ln f(x) dx \leq H(F,G)$ is the entropy of F. In this way, the measure $H(F,G)$ can be interpreted as the adequacy of the distribution G to predict an event

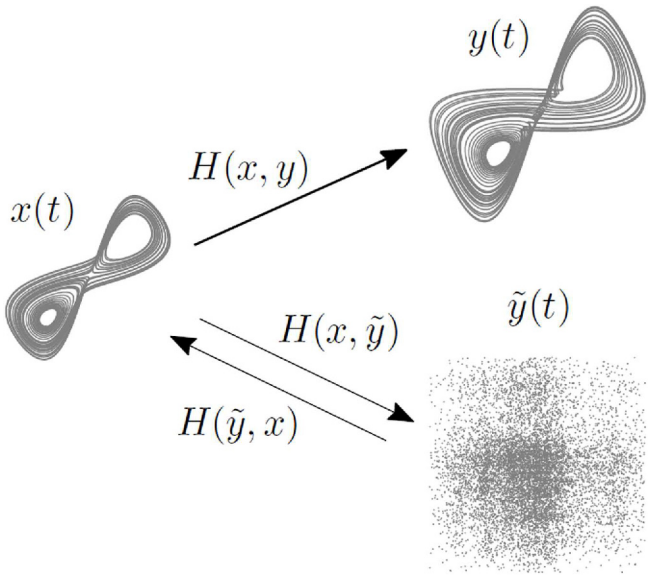

Fig. 2. Cross-entropy representation as a function of dimensionality. The reconstructed attractors are from the Lorenz system components: $\vec{x}(t) = M[x(t)]$ in the left plot; $\vec{y}(t) = M[y(t)]$ in the upper right plot; and $\tilde{\vec{y}}(t) = M[\tilde{y}(t)]$ in the bottom right plot. M is a embedding function. The lower cross-entropy value $H(x, y)$ is obtained when we consider two variables with the same dimension. This cross-entropy $H(x, \tilde{y})$ is higher than the previous, because the random data $\tilde{y}$ is less adequate to model the low dimensional data x. The worst scenario is characterized by the higher $H(\tilde{y}, x)$, when a low dimensional data is considered to model a higher-dimensional data.

from the distribution F. The maximum adequacy is reached when $D_{\mathrm{KL}}(F, G) = 0$, implying that G brings no new information in the prediction of F, since otherwise $H(F, G)$ would be greater than $H(F)$.

Instead of calculating the cross-entropy over probability distribution, it is calculated over the power spectrum (PS) of each signal, as in [21]. The PS is defined as $P(\omega) = |X(\omega)|^2$, where $X(\omega)$ is the Fourier transform of signal $x(t)$ and it is estimated using the method proposed in [22]. This method consists in dividing the time series into overlapping segments, calculating the PS for each segment and then averaging it over the segments. We propose to employ the normalized PS as the distribution, instead of using the signal amplitude, thus connecting the entropy with the rhythms/frequencies distribution from EEG data. In this sense, we can compare the energy contributions in frequency domain using the KLD.

To illustrate the cross-entropy concept, we consider the Lorenz system, defined by the equations: $dx/dt = \sigma(y - x)$, $dy/dt = x(\rho - z) - y$ and $dz/dt = xy - \beta z$, where $\sigma = 10$, $\beta = 8/3$ and $\rho = 28$. The simulation was evolved using a time step of 10^{-4}. In this case, we obtain $H(x, y) = 7.044$ and $H(x, \tilde{y}) = 9.519$, where $\tilde{y}$ is a shuffled random replica of y, and $H(\tilde{y}, x) = 21.040$. As expected, the lower value of cross-entropy was obtained for the two signals sharing the same generator mechanism. When using the random data $\tilde{y}$ as reference to evaluate the adequacy to predict an event in x, this measure increases and suggests an inadequacy of a stochastic process to predict the chaotic signal. The higher cross-entropy was obtained with a lower-dimensional data, x, as reference to evaluate the suitableness of prediction of the high-dimension data $\tilde{y}$. The toy model relationships are summarized in Figure 2.

An advantage of using the cross-entropy measure in a network is the global invariance. This property arises when we calculate the difference between the amount of

information from network to model a node, less the node accuracy to model all other remaining ones. In a specific node i, it is defined as $L_i = \sum_j (H_{ij} - H_{ji})$ where $H_{ij} = H(F_i, F_j)$. Thus, L_i can be interpreted as a relative measure of independence of a given node i. Regarding brain connectivity analysis, a significant value of $L_i > 0$ means a very dissimilar activity, which is composed by the brain rhythms and its combinations, from this node when compared to the network, while a low value $L_i < 0$ is attributed to more similarities with other nodes in frequency domain. The global invariance is then defined by the condition $\sum_i L_i = 0$, despite $L_i \neq 0$. This property can be interpreted as a reallocation of the cross-entropy while keeping the total amount of interactions constant.

3.2 Data Analysis

The multivariate EEG data was segmented in time windows w with 5 seconds with 80% overlap between them. Our analysis considered the brain rhythms in *delta*, *theta* and *alpha* domains (from 0.5 to 14 Hz). In each time window, the PS was estimated and normalized for each electrode. After this procedure, the cross-entropy was calculated between all pairs. An example of PS can be seen in Figure 3, where a well-known feature of absence seizures is the peak around 3–4 Hz (see Figs. 3b and 3d).

3.3 Detecting the significant nodes

Depending of measure used for network inference, different interpretations can be assigned to the structures unveiled, as for example, anatomical and functional hubs can be related with information flow (see [23]). Using cross-entropy as measure for network inference, we found two kinds of possible node states: independent and synchronizable nodes [24]. Independent node presents a dissimilar activity when compared to other nodes, characterized by strong capacity of not being influenced and establishing an important structure in the network. On the other hand, a synchronizable nodes i show a low L_i, due to a similarity among all PS, and a common information to model the phenomena. In order to check the significance of these nodes, a statistical test was performed for each time window w, consisting in the following steps:

- for each electrode i, calculate L_i;
- separate each L_i in two sets, one for $L_i > 0$ (independent) and another for $L_i < 0$ (synchronizable);
- normalize each L_i by the total of the respective set, resulting in a percentage information;
- for each normalized $L_i > 0$, do a left-sided Wilcoxon statistical test to verify if its contribution is larger than the median of the set. For $L_i < 0$ set, do a right-sided test.

With this procedure it is possible to find the regions that are significantly *distant* from the median of each set, highlighting the most independent and synchronizable sites in the network.

3.4 Phase-locking value

We employed the pairwise phase-locking value (PLV) as the synchronization measure between two signals to characterize the stability of the phase difference between two EEG data. PLV is a popular synchronization measure with well known properties.

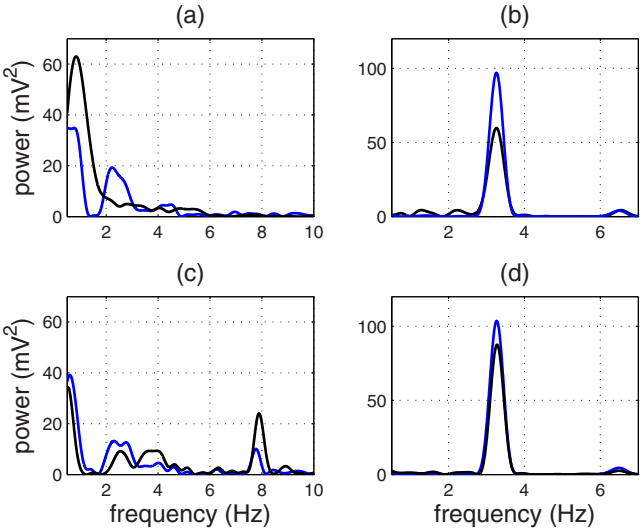

Fig. 3. Power spectra for two electrodes during interictal and ictal period. Figures (a) and (b) are the PS for frontal electrodes F3 (blue) and F8 (black) during interictal ($D_{\mathrm{KL}} = 0.787$; PLV $= 0.467$) and ictal ($D_{\mathrm{KL}} = 0.310$; PLV $= 0.625$) respectively, while the figures (c) and (d) are the PS estimated during interictal ($D_{\mathrm{KL}} = 0.418$; PLV $= 0.712$) and ictal ($D_{\mathrm{KL}} = 0.042$; PLV $= 0.916$) from central electrodes CZ (black) and PZ (blue), for the same time window used in the figures (a) and (b).

This method was successfully applied in a large number of EEG analysis, a recent comparison of PLV with other synchronization measures can be found in [25]. When the PLV is close to zero, the phase difference is uniformly identical and an unsynchronized state is identified. A PLV near to one, the phase difference is concentrated around preferred value frequencies, indicating a well established synchronization (see [26]). This measure is defined as

$$\mathrm{PLV}_{jk} = \frac{1}{N}\left|\sum_{i=1}^{N}\exp(\sqrt{-1}\Delta\varphi_{ijk})\right| , \tag{1}$$

where N is the window length, $\Delta\varphi_{ijk} = \phi_{ij} - \phi_{ik}$ with j and k representing two different electrodes and ϕ_{ij} is the mean phase weight-averaged energy for the electrode j in the time i. For more details see [27].

4 Results and discussion

4.1 During seizures, high values of cross-entropy are concentrated in few regions

A well defined pattern can be seen when comparing the matrices of pairwise cross-entropy inferred during ictal recordings with matrices from interictal periods (see for example the upper part of Fig. 4). During ictal period, most values are low and similar, except for few electrodes which have high values of cross-entropy, suggesting a very different electrophysiological activity in these electrodes. In other words, they have information which is not present in other regions. For this particular example, all regions (with exception of the frontoparietal area) exhibit uniform and low values of cross-entropy, an indicative of similar and synchronized activity.

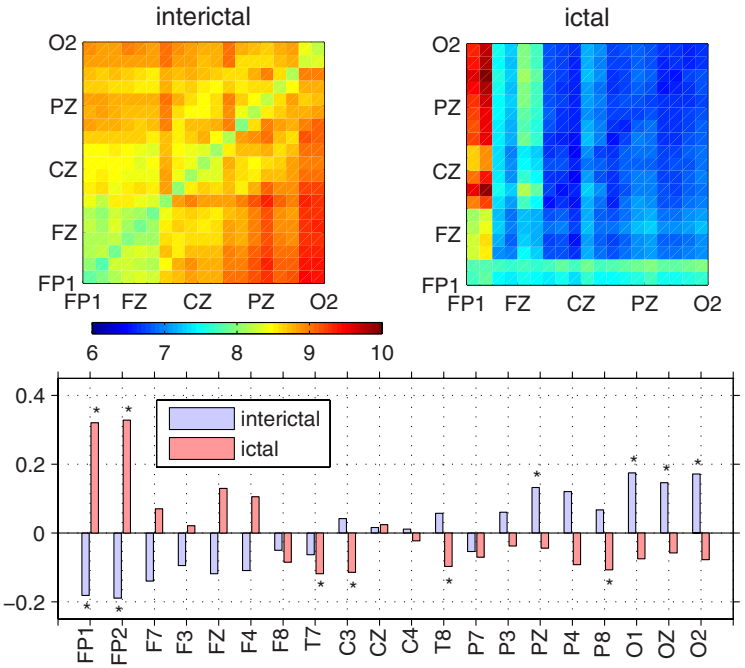

Fig. 4. Cross-entropy matrices for the patient S8. The upper frames are the average entropy matrices for the interictal (left) and ictal (right) periods during 7 seconds. The diagonal line is the entropy $H(\mathrm{PS}(\cdot))$ of each electrode. The bottom frame shows L_i for both periods. We observed two independent nodes in the frontoparietal area (FP1 and FP2 electrodes) during the ictal period. Four independent nodes were observed for the interictal period (PZ, O1, OZ and O2 electrodes), but with lower cross-entropy than the independent nodes from ictal period. The electrodes FP1 and FP2 were classified as synchronizable nodes in the interictal period and the number of these nodes increases during the seizure (T7, C3, T8 and P8).

The matrix from interictal period shows high values of cross-entropy between signals, but they are less prominent and dispersed across brain regions, indicating that different regions are performing different activities in opposition to the matrix inferred during the ictal period. The most important regions for both periods can be seen in the bottom panel of Figure 4. In this plot, each bar is the L_i for each electrode i and the marker (denoted by $*$) points to those which have greater or smaller values of L. We can see that during the ictal period electrodes FP1 and FP2, can be classified as independent, since they concentrate most part of the total of $L > 0$. On the other hand, the electrodes T7, C3, T8 and P8 were classified as synchronizable. These are the most significant nodes among those who have $L < 0$.

Table 1 presents a summary of results for the eight subjects. It is important to notice an increase of L from interictal to ictal periods. Although the number of independent nodes were higher during interictal, these nodes are more prominent in the ictal period, concentrating most part of the nodes with $L > 0$. Furthermore, the number of synchronizable nodes increases during the seizure, suggesting a necessary condition to achieve brain hypersynchronization.

4.2 The significant nodes exhibit a well defined dynamical pattern

Both matrices from Figure 4 are temporal average of cross-entropy: the right one is from an ictal period of 7 seconds and the left is the matrix for the same time

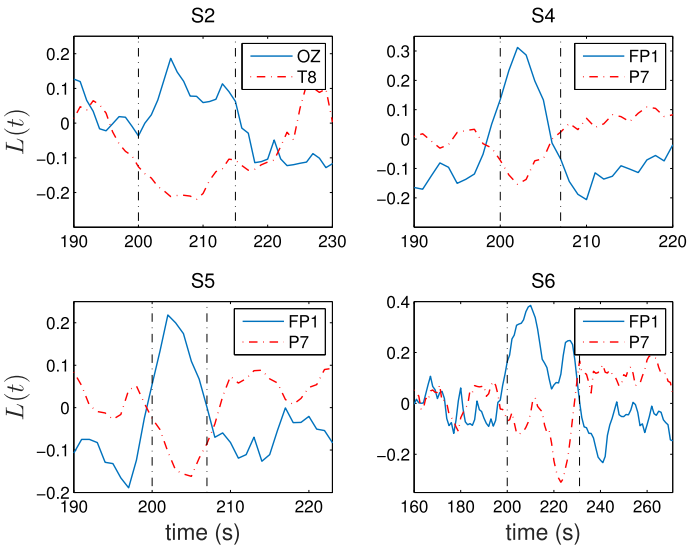

Fig. 5. Measure L as a function of time for independent (solid blue) and sychronizable (dashed red) nodes from four patients with different seizures duration. Dashed vertical lines indicate the seizure onset and termination.

Table 1. Number of significant nodes for interictal and ictal periods. L_i-positive (-negative) average is indicated by $\overline{L}_+$ ($\overline{L}_-$). Was considered a significance level of 0.05 for Wilcoxon test application. No synchronizable nodes were observed for S5 due to low number of nodes with $L_i < 0$, in this case we choose the more effective. $\Delta\overline{D}_{\mathrm{KL}}\%$ is the percentage variation of averaged KLD (from interictal to ictal), measured only among the independent nodes detected during ictal period.

	Interictal period				Ictal period				
Subject	#ind	$\overline{L}_+$	#syn	$\overline{L}_-$	#ind	$\overline{L}_+$	#syn	$\overline{L}_-$	$\Delta\overline{D}_{\mathrm{KL}}\%$
S1	4	0.101	1	−0.311	2	0.274	2	−0.241	−35.85
S2	2	0.200	3	−0.200	2	0.235	4	−0.131	−74.41
S3	4	0.135	3	−0.227	4	0.139	4	−0.189	−52.34
S4	3	0.140	1	−0.505	2	0.381	3	−0.139	−85.33
S5	5	0.100	2	−0.300	2	0.264	3	−0.197	−82.93
S6	3	0.193	1	−0.313	2	0.358	4	−0.139	−96.22
S7	5	0.110	2	−0.273	1	0.334	5	−0.119	–
S8	4	0.160	2	−0.198	2	0.321	4	−0.106	−77.37

duration just before the seizure onset. In order to analyze the dynamical behaviour of L, we show in Figure 5 this measure as a function of time for independent and synchronizable nodes. For the former, $L(t)$ reaches its peak during the ictal period and progressively decreases afterwards, while $L(t)$ shows an inverse behaviour for the synchronizable nodes. After the ictal period, the measure $L(t)$ returns to the same level observed before seizure onset. The dynamics of these nodes suggests a complementary role between the independent and synchronizable nodes during the seizure period.

4.3 The independent nodes are less synchronized

Considering only the KLD measure, the global network synchronization is more expressive during seizure. In order to compare this measure from different time

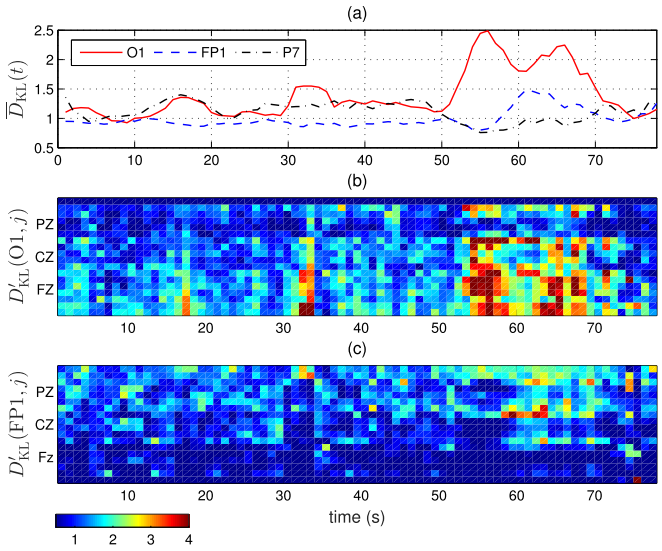

Fig. 6. Pairwise KLD between all electrodes for one subject. (a) $\overline{D}_{\mathrm{KL}}(t)$ measure for three electrodes. Synchronization level for the electrodes (b) O1 and (c) FP1 for each electrode. The ictal period is comprised in the time interval 50 to 70 seconds.

windows, we normalized the KLD matrix by its mean, as expressed by

$$D'_{\mathrm{KL}}(i,j) = \frac{n^2 D_{\mathrm{KL}}(i,j)}{\sum_{i=1}^{n}\sum_{j=1}^{n} D_{\mathrm{KL}}(i,j)} \ , \tag{2}$$

where n is the number of electrodes. Thereby, we can measure how much the electrode i is unsynchronized from the electrode j, having the network synchronization as reference, as discussed in Section 3.1.

Figure 6a shows the $\overline{D}_{\mathrm{KL}}(i) = 1/n \sum_{j=1}^{n} D'_{\mathrm{KL}}(i,j)$ of three selected electrodes during the seizure of one subject: O1 which is an independent node and the synchronizable nodes P7 and FP1. Before seizure onset, they present a resembling regime sharing a same baseline. After seizure onset $\overline{D}_{\mathrm{KL}}(\mathrm{O1})$ increases, remaining higher than the others two until the seizure end, when it returns to baseline. For FP1 and P7, this function decays after seizure onset, suggesting a synchronization state of the brain network with these nodes. Figure 6b presents the $D'_{\mathrm{KL}}(\mathrm{O1}, j)$ for each other electrode j and analogously in Figure 6c it is the same measure for FP1. We can observe that after the seizure onset $D'_{\mathrm{KL}}(\mathrm{FP1}, j)$ indicates a similar activity with all the network nodes, excepting with the occipital nodes (which are classified as independent). For a more complete description of dynamical properties of the synchronization during seizures see Rodrigues et al. [28].

Furthermore, the independent nodes during ictal period shows a low KLD (high synchronization) between them, indicating that there are at least two oscillatory regimes in the network: one shared by all non independents nodes and another for a subnetwork formed by the independents. This KLD difference observed on independent nodes between pre-ictal and ictal periods can be seen in Table 1 and suggests a more synchronized activity between these nodes.

5 Conclusions

This paper proposes the use of cross-entropy in frequency domain, that was applied to EEG signals acquired from patients with absence seizures, as a connectivity

estimation for multivariate neural data. The results portray an interesting description for this kind of seizure, revealing not only local patterns of regions that aren't synchronized with the network but also showing its dynamical interactions. We propose a classification scheme for the regions based on its features during the seizures: independent nodes, those which present a different activity when compared to other nodes from network; and the synchronizable nodes, which in turn are those with similar (and consequently synchronized) activity. One remarkable local pattern was the temporal evolution of measure L for independent and synchronizable nodes, whereas the former has a peak of maximum cross-entropy on the course of seizure, the latter shows a minimum.

These findings bring some questions about the nature of seizure spreading: i) What is the role of the independent nodes? ii) Are they part of an active mechanism to inhibit the seizure or are they contributing to spreading? The later hypothesis presumes an active role of these nodes. Then if they are a consequence of spreading mechanism, they are not able to cover all regions with the same oscillatory pattern. The two hypotheses can possibly lead to a similar behaviour as seen in this work. In this way, the occurrence of a second oscillatory pattern can be related with inhibition or spreading mechanisms originated from effects of interference or superposition between the brain waves.

In addition, this paper shows the importance of taking into account not only one kind of interaction between signals, as causal relationships, but also the other types of interactions, as dissimilarity [29] and the ones presented here. Neglecting brain regions without direct causal relation can lead to an incomplete model of the process. It is important to notice that a dissimilar activity in slow rhythms, observed in entropy matrices inferred from the interictal periods, is a remarkable feature in brain cognitive processing [30,31]. Moreover, due the dynamical behaviour observed in the regions, which can change its role along time, the independent nodes can be synchronizable nodes in seizure-free intervals. We believe that changes between roles can be related with the synchronization and others emergent phenomena.

ACR thanks CAPES and UNIEMP; HAC thanks ICTP-SAIFR and FAPESP grant 2011/11973–4; and BSM thanks UNIEMP.

References

1. D. Rangaprakash, N. Pradhan, Biomed. Signal Process. Control **11**, 114 (2014)
2. T.I. Netoff, S.J. Schiff, J. Neurosci. **22**, 7297 (2002)
3. A. Sanz-García, R.G. de Sola, L. Vega-Zelaya, J. Pastor, G.J. Ortega, Network theoretical approach to describe epileptic processes, in *Advanced Biosignal Processing and Diagnostic Methods*, edited by C. Hintermüller (InTech, Viena, 2016)
4. F. Mormann, T. Kreuz, R.G. Andrzejak, P. David, K. Lehnertz, C.E Elger, Epilepsy Res. **53**, 173 (2003)
5. F. Wendling, F. Bartolomei, J.J. Bellanger, J. Bourien, P. Chauvel, Brain **126**, 1449 (2003)
6. K. Schindler, H. Leung, C.E. Elger, K. Lehnertz, Brain **130**, 65 (2007)
7. P. Jiruska, M. de Curtis, J.G. Jefferys, C.A. Schevon, S.J. Schiff, K. Schindler, J. Physiol. **591**, 787 (2013)
8. V. Volman, M. Perc, M. Bazhenov, PLoS One **6**, e20572 (2011)
9. D. Fan, W. Qingyun, M. Perc, Sci. Rep. **5**, 12618 (2015)
10. C.A. Schevon, R.R Goodman, G. McKhann Jr R.G. Emerson, J. Clin. Neurophysiol. **27**, 406 (2010)
11. M. Stead, M. Bower, B.H. Brinkmann, K. Lee, W.R. Marsh, F.B. Meyer, B. Litt, J. Van Gompel, G.A. Worrell, Brain **133**, 2789 (2010)

12. M. Bikson, J.E. Fox, J.G. Jefferys, J. Neurophysiol. **89**, 2330 (2003)
13. M. Le Van Quyen, J. Martinerie, V. Navarro, M. Baulac, F.J. Varela, J. Clin. Neurophysiol. **18**, 191 (2001)
14. E. Sitnikova, G. van Luijtelaar, Epilepsy Res. **84**, 159 (2009)
15. F. Amor, S. Baillet, V. Navarro, C. Adam, J. Martinerie, M. Le van Quyen, Neuroimage **45**, 950 (2009)
16. E. Visani, G. Varotto, S. Binelli, L. Fratello, S. Franceschetti, G. Avanzini, F. Panzica, J. Clin. Neurophysiol. **121**, 318 (2010)
17. D. Takeshita, Y.D. Sato, S. Bahar, Phys. Rev. E **75**, 051925 (2007)
18. S. Panahi, Z. Aram, S. Jafari, J. Ma, J.C. Sprott. Chaos Soliton. Fract. **105**, 150 (2017)
19. L.E. Martinet, G. Fiddyment, J. Madsen, E. Eskandar, W. Truccolo, U. Eden, S.S. Cash, M.A. Kramer, Nature Commun. **8**, 14896 (2017)
20. J. Shore, R. Johnson, IEEE Trans. Inform. Theory **26**, 26 (1980)
21. R.Q. Quiroga, J. Arnhold, K. Lehnertz, P. Grassberger, Phys. Rev. E **62**, 8380 (2000)
22. P.D. Welch, IEEE Trans. Audio Electroacoust. **15**, 70 (1967)
23. M.P. van den Heuvel, O. Sporns, Trends Cogn. Sci. **17**, 683 (2013)
24. J. Lunze, J. Phys. A **44**, 045103 (2010)
25. E. Lowet, M.J. Roberts, P. Bonizzi, J. Karel, P. De Weerd, PLoS One **11**, e0146443 (2016)
26. M. Chavez, M. Valencia, V. Latora, J. Martinerie, Int. J. Bifur. Chaos **20**, 1677 (2010)
27. V.S.G. Martins, A.C. Rodrigues, H.A. Cerdeira, B.S. Machado, Eur. Phys. J. Special Topics **225**, 41 (2016)
28. A.C. Rodrigues, B.S. Machado, G. Florence, A.P. Hamad, A.C. Sakamoto, A. Fujita, L.A. Baccalá, E. Amaro Jr K. Sameshima, Eur. Phys. J. Special Topics **223**, 2933 (2014)
29. G.J. Goodhill, M.W. Simmen, D.J. Willshaw, Philos. Trans. R Soc. Lond. B Biol. Sci. **348**, 265 (1995)
30. T. Koenig, L. Prichep, T. Dierks, D. Hubl, L.O. Wahlund, E.R. John, V. Jelic, Neurobiol. Aging **26**, 165 (2005)
31. C.J. Stam, Clin. Neurophysiol. **116**, 2266 (2005)